Accepted Manuscript

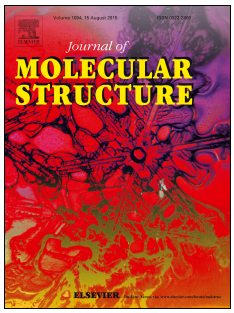

Copper(II) complex of new non-innocent *O*-aminophenol-based ligand as biomimetic model for galactose oxidase enzyme in aerobic oxidation of alcohols

Elham Safaei, Hadiseh Bahrami, Andrej Pevec, Bojan Kozlevčar, Zvonko Jagličić

PII: S0022-2860(16)31263-7

DOI: 10.1016/j.molstruc.2016.11.076

Reference: MOLSTR 23177

To appear in: *Journal of Molecular Structure*

Received Date: 2 October 2016

Revised Date: 24 November 2016

Accepted Date: 25 November 2016

Please cite this article as: E. Safaei, H. Bahrami, A. Pevec, B. Kozlevčar, Z. Jagličić, Copper(II) complex of new non-innocent *O*-aminophenol-based ligand as biomimetic model for galactose oxidase enzyme in aerobic oxidation of alcohols, *Journal of Molecular Structure* (2016), doi: 10.1016/j.molstruc.2016.11.076.

Copper(II) Complex of New Non-innocent *0*-aminophenol-based Ligand as Biomimetic Model for Galactose oxidase Enzyme in Aerobic Oxidation of Alcohols

Synthesis and characterization of copper complex of N_3O *0*-aminophenol based ligand as model for galactose oxidase in aerobic oxidation of alcohols have been investigated.

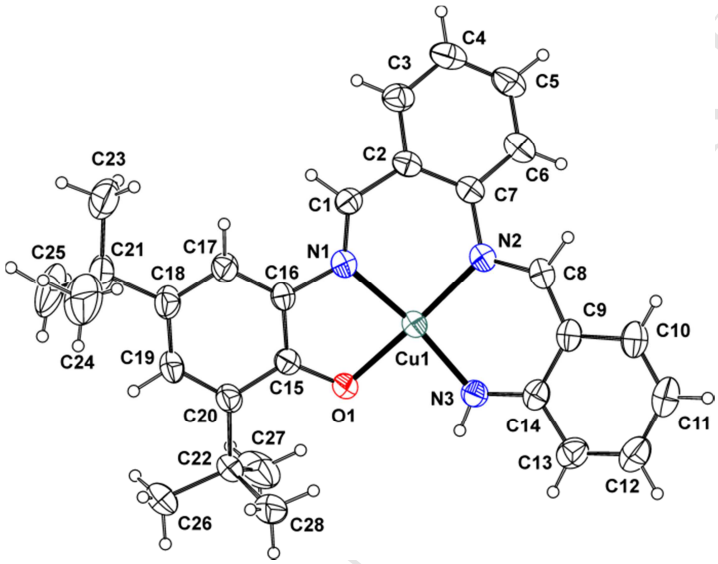

Copper(II) Complex of New Non-innocent *O*-aminophenol-based Ligand as Biomimetic Model for Galactose oxidase Enzyme in Aerobic Oxidation of Alcohols

Elham Safaei*[a] , Hadiseh Bahrami[b], Andrej Pevec[c], Bojan Kozlevčar [c], Zvonko Jagličić [d, e]
[b]Department of Chemistry, College of Sciences, Shiraz University, Shiraz, 71454, Iran
[a]Institute for Advanced Studies in Basic Sciences (IASBS), 45137-66731, Zanjan, Iran
[c]Faculty of Chemistry and Chemical Technology, University of Ljubljana,Večna pot 113, SI-1000 Ljubljana, Slovenia
[d]Institute of Mathematics, Physics and Mechanics, Jadranska c. 19. SI-1000, Ljubljana, Slovenia
[e]Faculty of Civil and Geodetic Engineering, Jamova c. 2. SI-1000, Ljubljana, Slovenia

Correspondence to: Elham Safaei

E-mail:e.safaei@shirazu.ac.ir

Abstract

Mononuclear copper(II) complex of tetra-dentate *o*-aminophenol-based ligand (H_2L^{BAPP}) has been synthesized and characterized. The three dentate precursor (HL^{BAP}) of the final ligand was synthesized first, while the title four-dentate copper bound ligand was synthesized in situ, isolated only in the final copper species [CuL^{BAPP}]. This copper coordination complex reveals a distorted square-planar geometry around the copper(II) center by one oxygen and three nitrogen atoms from the coordinating ligand. The ligand is thus twice deprotonated via hydroxy and amine groups. The complex is red, non-typical for copper(II), but the effective magnetic moment of 1.86 B.M. and a single isotropic symmetry EPR signal with g 2.059 confirm a S =1/2 diluted spin system, without copper-copper magnetic coupling. Electrochemical oxidation of this complex yields the corresponding Cu(II)–phenoyl radical species. Finally, the title complex CuL^{BAPP} has shown good and selective catalytic activity towards alcohol to aldehyde oxidation, at aerobic room temperature conditions, for a set of different alcohols.

Keywords: Galactose oxidase; Biomimetic copper complexes; Phenoxyl radical; Alcohol oxidation.

1. Introduction

Galactose oxidase (GO) is an important example of oxidoreductase enzymes that catalyze oxidation of D-galactose with simultaneous reduction of molecular oxygen to water or hydrogen peroxide. Within the active site of this enzyme, the synergistic action between copper and phenoxyl radical of cysteine-modified Tyrosine 272 residue has a critical role in the catalytic cycle (Scheme 1) [1-4].

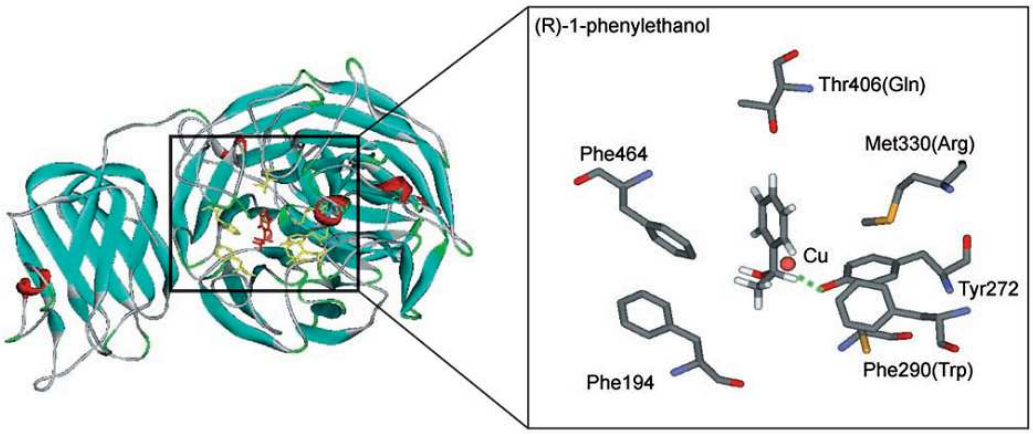

Scheme 1. Galactose oxidase (GO)active site [5]

It has been shown that GO passes three important oxidation levels, including metal radical species, during the catalytic cycle (Schemes 2, 3) [5-9].

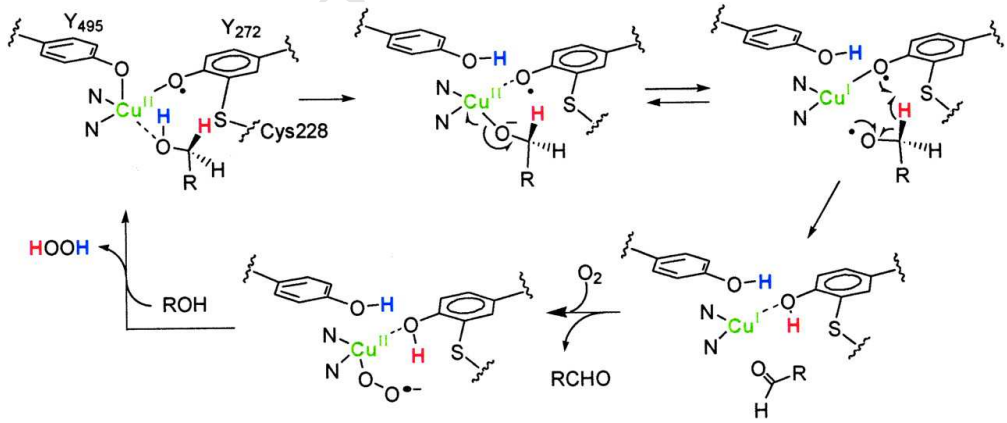

Scheme 2. Proposed mechanism for alcohol catalysis to aldehyde and hydrogen peroxide byGO [4].

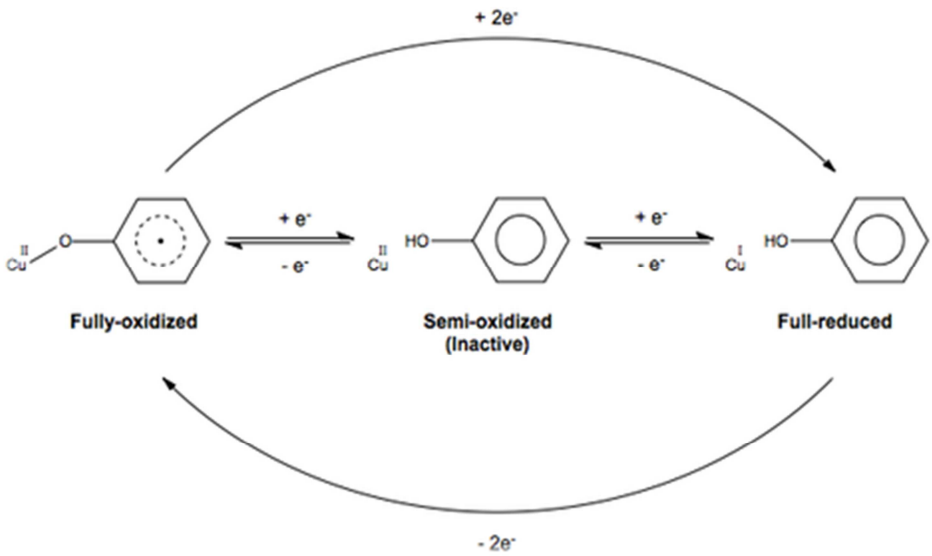

Scheme 3: Redox states of phenolate/copper in GO active site [7]

The discovery of the mentioned unusual biological entities, namely M…R$^{\bullet}$ such as copper - phenoxyl radical of Tyrosine 272 residue , in the active site of GO and similar species in other enzymes such as cytochrome P_{450}, has encouraged scientists to mimic the oxidative chemistry of complexs involving *o*-aminophenolates [10-14]. The involved ligands are known as a class of redox-active, 'non-innocent' ligands, the later term being focused onto metal-ligand coordination via different oxidation states (Scheme 4) [15-17]. *O*-aminophenols are one of the most common classes of redox active ligands. They can be bound to the transition metal ion with three oxidation forms, either as an *o*-aminophenolate dianion, *o*-iminobenzosemiquinonate π radical monoanion and neutral iminoquinonate ligand.

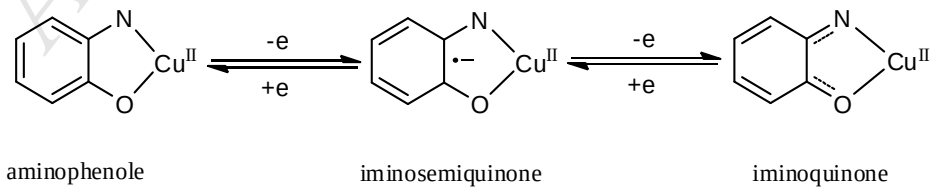

Scheme 4: Redox state of redox active ligands [17]

Copper complexes based on 'non-innocent' catecholate and semiquinones ligands have also been identified as GO-like reactive [17-20]. The oxidation of alcohols to aldehydes is one of the considerably interest reactions in organic chemistry [21-23]. A ligand–assisted Cu catalytic system containing copper employing pyridine or bipyridine ligands [24] was reported to catalyze the selective aerobic oxidation of alcohols to aldehydes. The catalytic oxidation of alcohols to aldehydes, based on the isolated Cu complexes, has been also reported by several groups [25-32].

In this work, we reveal a design of a mononuclear copper complex with in situ prepared 'non-innocent *o*-aminophenole N_3O based ligand (Scheme 5). Subsequently, its performance as efficient catalytic system for the aerobic oxidation of benzyl alcohols was investigated.

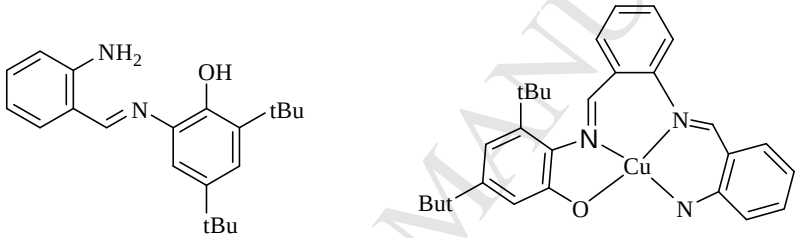

Scheme 5 . Structure of the precursur ligand HL^{BAP} and copper complex CuL^{BAPP}

2. Experimental

2.1. Materials and physical measurements

Reagents or analytical grade materials were obtained from commercial suppliers and used without further purification, except those for electrochemical measurements. Elemental analyses (C, H, and N) were performed by the Elementar, Vario EL III . Fourier transform infrared spectroscopy with KBr pellets was performed on a FT IR Bruker Vector 22 instrument. NMR measurements were performed on a Bruker 400 instrument. UV-Vis absorbance digitized spectra were collected using a CARY 100 spectrophotometer. The electronic absorption spectra of complexes have been measured in dichloromethane in the 200-800 nm range.

Crystal data and refinement parameters of complex CuL^{BAPP} are listed in Table 1. The X-ray diffraction data were collected at room temperature on an Agilent Technologies SuperNova Dual source diffractometer with an Atlas detector using mirror-monochromatized Mo Kα radiation (λ = 0.71073 Å). The data were processed using CRYSALIS PRO[33]. The structures were solved by direct methods implemented in SIR–92 [34] and refined by a full-matrix least-squares procedure based on F^2 using SHELXL–97 [35]. All non-hydrogen atoms were refined anisotropically. All hydrogen atoms bonded to carbon (except C1 and C8) were included in the model at geometrically calculated positions and refined using a riding model. The N–bound hydrogen atoms were located in a difference map and refined with the using distance restraints (DFIX) with N–H = 0.86 and with Uiso(H) = 1.2U_{eq}(N). The C1– and C8–bound hydrogen atoms were located in a difference map and refined with the using distance restraints (DFIX) with C–H = 0.98 and with Uiso(H) = 1.2U_{eq}(C).

Table 2

Magnetic susceptibility was measured with powder sample in the temperature range 2-300 K by using a SQUID magnetometer (Quantum Design MPMS-XL-5) in a magnetic field of 1000 Oe. EPR spectra were collected using a Bruker EMX plus spectrometer operating with a premium X X-band (~9.5 GHz) microwave bridge. Low temperature measurements of frozen solutions used a Bruker helium temperature-control system and a continuous flow cryostat. Voltammetric measurements were made by a computer controlled electrochemical system (ECO Chemie) equipped with a PGSTA 30 model and driven by GPES (ECO Chemie). A glassy carbon electrode, with a surface area of 0.035 cm^2, was used as a working electrode, while a platinum wire served as a counter electrode. The reference electrode was a silver wire as the pseudo reference electrode. Ferrocene was added as an internal standard after completion of a set of experiments, and potentials are referenced vs. the ferrocenium/ferrocene couple (Fc^+/Fc).

2.2. Synthesis

Synthesis of HL^{BAP}

A synthesis of ligand precursor HL^{BAP} (Scheme 6) was already previously described [16, 36]. A solution of 3,5-DTBQ (3,5-di *tert* butyl quinone; 0.22 g, 1.0 mmol) in acetonitrile (4 mL) was prepared, to which 2-aminobenzyl amine (0.122 g, 1.0 mmol) was added. The reaction solution was stirred for 30 min at the room temperature in the presence of air. The yellow precipitate of HL^{BAP} was filtered off and dried in air.

(0.278 g, 85% yield). Anal. Calcd. for $C_{21}H_{28}N_2O$ (324.46 g/mol) C, 77.74; H, 8.70; N, 8.63%. Found: C, 76.93; H, 8.55; N, 8.48%. ^{1}H NMR (400 MHz, $CDCl_3$, 298 K): δ 1.4(s, 9H), 1.5(s, 9H), 6.3(s, 2H), 6.7 (s, 1H), 6.8(m, 2H), 7.0 (d, 1H), 7.3(d, 2H), 7.4 (d, 1H), 8.7(s, 1H). ν_{max}(KBr)/cm^{-1}: 3421 (O–H, N–H); 2951(C–H); 1466 (C–H), 1212 (C–O), 1607 (C=N) 651(C-H, methylene). ESI-MS m/z (%): 325.5 $[M_{HL^{BAP}+1}]^+$.

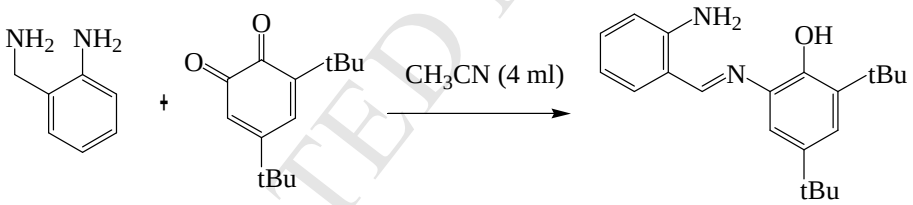

Scheme 6. Synthesis pathway of the precursor ligand H_2L^{BAP}.

Synthesis of the complex $[CuL^{BAPP}]$

Methanol (50 mL) was added to powdered **1** (0.324 g, 1.0 mmol) and proline (0.115 g, 1.0 mmol). After one minute of stirring, Cu $(OAc)_2\cdot(H_2O)$ (0.199 g, 1.0 mmol) and of NEt_3 (0.199 g, 1.0 mmol) were added into the initial reaction mixture, while the color turned to red-brown. After 4 h at 298 K, a red-brown microcrystalline precipitate of CuL^{BAPP} was filtered off. It was dried under air. (0.351 g, 72% yield). X-ray quality dark red single crystals were grown from a 1:1 (V:V) dichloromethane/ethanol. Elemental Analysis:

calculated (found) for $C_{28}H_{31}CuN_3O$ (489.1 g/mol): C; 72.34, H; 7.31, N; 8.61, Cu; 10.2; Found: C; 71, H; 7.24, N; 8.57, Cu; 9.7. ν_{max}(KBr)/cm^{-1}: 2949 (C-H), 1628 (C=N), 1612 (C=N), 1466 (C=C), 808 (=C-H bending). ESI-MS m/z (%): 489.5 $[M_{HL+Cu}]^+$, 878.5 $[M_{HL+Cu}]_2^+$.(Figure 4S).

Catalytic activity of [CuL^{BAPP}]

In a typical experiment, alcohol (1.0 mmol), [CuL^{BAPP}] (4 mmol%), Cs_2CO_3 (0.650 g, 2 mmol) and 5 mL THF (oxygen saturated) were inserted in a 25 mL two-necked round-bottom flask, equipped with an oxygen balloon. The solution was stirred at room temperature, after which the mixture was filtered through a plug of silica, and then diluted with THF (2 mL). The progress of the reaction was monitored by gas chromatography. For a comparison, blank tests were performed, with the identical flask and amounts of Cs_2CO_3, THF (oxygen saturated) and oxygen balloon. Instead of CuL^{BAPP}, only copper(II) acetate, or precursor ligand HL^{BAP} were used.

3. Results and Discussion

The copper(II) complex CuL^{BAPP} was synthesized by the reaction of the precursor ligand HL^{BAP} with copper acetate in the presence of proline in methanol (Scheme 7). During the synthesis, several possible reactions seem to appear (Scheme 8), with the final in situ ligand H_2L^{BAPP}, being found only coordinated in CuL^{BAPP}, where it is in a double deprotonated form. It is worth to note that in the absence of proline, the product CuL^{BAPP} wasn't isolated pure, but the insoluble solid mixture precipitated instead, which we were unable to characterize. Therefore, we decided to add other ligand as capping agent prevent a possible polymerization process. In addition, in the presence of glycine and tyrosine amino acids the same product as proline was produced.

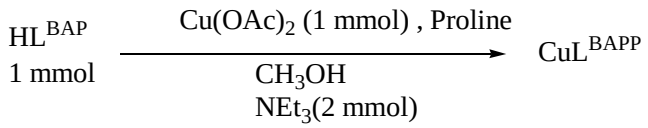

Scheme 7. The synthesis pathway of copper(II) complex CuL^{BAPP}

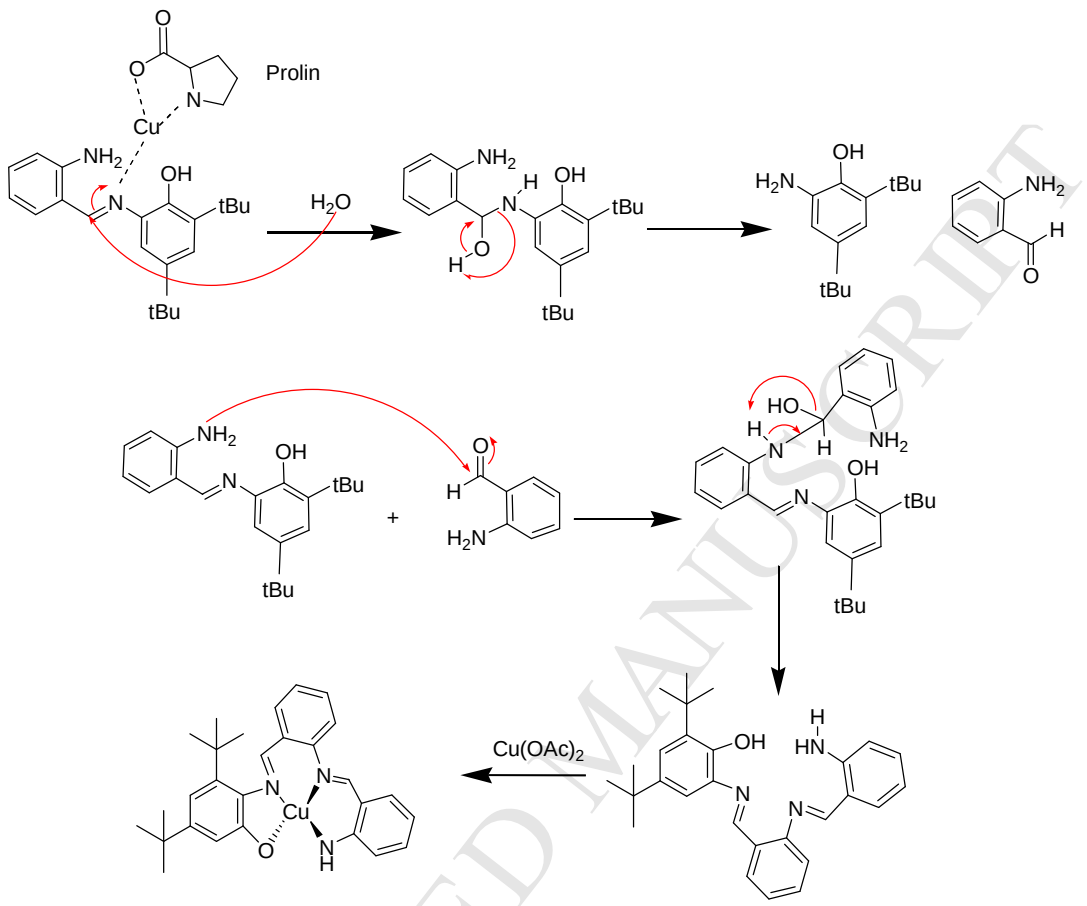

Scheme 8. The suggested reaction pathway for the synthesis of CuL^{BAPP} and the in situ ligand H_2L^{BAPP} from HL^{BAP}

3.1. The crystal structure description for CuL^{BAPP}

The complex [CuL^{BAPP}] crystallizes in the monoclinic space group *C*2/*c*, with one formulae within the asymmetric unit (Figure 1). The geometry of the coordination sphere is square-planar, with tetradentate *o*-aminophenol-based ligand HL^{BAP} binding the central Cu(II) through one oxygen atom and three nitrogen atoms. A coordination of the asymmetric [N_3O] ligand to the copper(II) ion generates three chelate rings, two of them composed by six atoms and the other one by five atoms. The C–C, C–O and C–N distances in the six- and five-

membered rings within the structure of CuL^{BAPP} are in accordance with the distances in the complex with the similar structural fragment thus indicating delocalization of electron density over these rings. There is also no evidence for any significant non-covalent interactions. Selected bond lengths and angles for the CuL^{BAPP} are given in Table 2.

Figure 1

Table 2

In the IR spectrum of *CuL^{BAPP}*, a deprotonation and coordination of the ligand H_2L^{BAPP} phenol and amine groups are in agreement by the replacement of the strong and sharp bands seen in the spectrum of HL^{BAP} (precursor ligand to H_2L^{BAPP}) around 3300-3500 cm^{-1}, by a broad band found in the spectrum of *CuL^{BAPP}. The ν(C = N) band found for CuL^{BAPP} at 1612 cm^{-1} is shifted to higher frequencies from 1607 in* HL^{BAP}*, also indicating the ligand coordination via the azomethine nitrogen atom* .

In the UV-Vis spectrum of CuL^{BAPP}, two absorption bands at 508, 409, 340 and 273 nm are seen. The visible region band is assigned to phenolate (π) -to- Cu(II) (dπ*) charge transfer (LMCT). On the other hand the UV region band is assigned to ligand π→π* transitions of phenolate units (Figure 2) [37].

Figure 2

The MS spectrum of CuL^{BAPP} shows an intense ion peak with molecular weight of 489.5 related to a complex containing copper and a rearranged ligand so as three dentate HL^{BAP} ligand reacts with 2-amino benzaldehyde species(from hydrolysis of aminobenzyl amine) and produce four dentate H_2L^{BAPP} ligand which clearly indicated the formation of 1:1 complex $[M_{H_2L^{BAPP}}+Cu]^+$. X-ray analysis confirms this proof. Another peak placed at 878.5 is related to a dimeric form of copper complex. The molecular peak of the complex ion is shown in the supplementary materials. The suggested reaction pathway for the synthesis of CuL^{BAPP} has been shown in Scheme 8. We didn't observe proline or other above mentioned amino acids in

the structure of complexes and all synthesized complexes show the same mass spectrum pattern. It considers that amino acids play a catalytic rule in hydrolysis of HL^{BAP} and formation of H_2L^{BAPP}.

3.2. Magnetic susceptibility

Temperature variation of measured molar magnetic susceptibility $\chi_M(T)$ for CuL^{BAPP} is shown in Figure 3. The presented data were corrected for the temperature-independent Larmor diamagnetic susceptibility obtained from Pascal's tables [38] and for the sample holder contribution. The susceptibility of CuL^{BAPP} increases with decreasing temperature, following a Curie 1/ T law, which indicates a paramagnetic behavior (Figure 4). Almost temperature independent effective magnetic moment of copper complex confirms proposed paramagnetic property of this mononuclear species. The effective magnetic moment (Figure 3) at room temperature is around 1.86 BM, being very close to the measured values for the other diluted copper complexs (reported values in [39] are 1.77–1.83 BM). This is in agreement with the presence of one unpaired electron and quantum spin number S = ½ in the copper center of complex. Susceptibility graph $\chi_M^{-1}(T)$ shows a straight line of slope *1*/C passing through the origin (0 K). Only a small downturn of the effective magnetic moment below 20 K may indicate a weak antiferromagnetic interaction between the Cu(II) centers.

Figure 3

Figure 4

3.3. EPR spectroscopy

Frozen solution EPR shows a single isotropic symmetry signal with a g value of 2.059. It is more than the free electron g value (2.0023) attributed to a single-electron copper(II) d^9 configuration. A typical EPR spectrum of CuL^{BAPP} has been shown in Figure 5.

Figure 5

3.4. Electrochemistry

Cyclic voltammogram (CV) of CuL^{BAPP} has been recorded by CH_2Cl_2 solution containing 0.1 M $[(n\text{-Bu})_4N]ClO_4$ as a supporting electrolyte. It displays two pseudo-reversible anodic redox processes at 0.630 and 0.825 V, indicating a ligand-centered oxidation to form phenoxyl radical species (*vide infra*). Both oxidation potentials are comparable to the first oxidation potential reported for a large number of Cu^{II}-imino-phenolate complexes (~0.45 V vs. Fc^+/Fc in CH_2Cl_2), that exhibit ligand radical formation [40-44]. The redox process at -1.25 V could be a Cu^{II}/Cu^{I} reduction process based on previously reported data [40-44]. Cyclic voltammogram (CV) of CuL^{BAPP}, is presented in Figure 6.

Figure 6

3.5. The catalytic activity of CuL^{BAPP}

To study the application of CuL^{BAPP} for the aerobic oxidation of alcohols to corresponding aldehydes, benzyl alcohol was chosen as a model complex and the reaction conditions were optimized accordingly. The initiation time was around half an hour (Fig. 7).

Figure 7

Various organic solvents were used to determine the optimal one. The THF appeared to be the most favorable for the described transformation (Table 3) and not fluorinated solvents, which are usually used in such cases [45].

Table 3

The catalyst CuL^{BAPP} optimal quantity was 4.0 mmol%, when 4 h were needed for the complete transformation (Table 4).

Table 4

Additionally, different bases for oxidation of benzyl alcohol were checked, with. 2 equivalents of Cs_2CO_3 optimally used Cs_2CO_3 (Table 5).

Table 5

The ligand-free copper(II) acetate/Cs_2CO_3 blank test shows an appearance of aldehyde in low yield (Scheme 6, Table 6). On the other hand, copper(II) acetate/Cs_2CO_3, in the presence of ligand precursor HL^{BAP}, increases the aldehyde yield. This suggests the ligand effect on increasing alcohol conversion. Comparing these results with the analogous for [CuL^{BAPP}/Cs_2CO_3], suggests us to include the metal-ligand synergy role into the oxidation of alcohols. Under optimized reaction conditions (4 mmol % of CuL^{BAPP}, 2 mmol Cs_2CO_3, THF as solvent), namely, various substituted benzaldehydes were obtained from their corresponding, alcohols (Table 7).

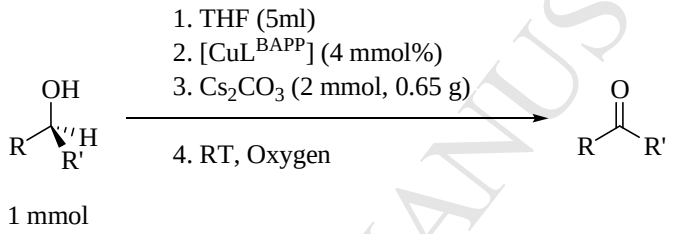

Scheme 6. Catalytic activity of CuL^{BAPP} at the aerobic oxidation of alcohols

Table 6

These results also reveal that unsubstituted benzylic alcohols are oxidized more efficiently than aliphatic alcohols. Further oxidation towards the corresponding acids was not observed (Scheme 6).

Table 7

4. Conclusion

In summary, a new square-planar copper(II) complex CuL^{BAPP} with the in situ prepared aminophenol-based ligand H_2L^{BAPP} was synthesized and characterized. Electrochemical oxidation of this copper complex yields the corresponding Cu**(**II**)–**phenyl radical species. In addition, highly efficient and eco-friendly oxidation of alcohol to aldehyde was achieved with molecular oxygen as an oxidant and non-expensive catalyst system CuL^{BAPP} /Cs_2CO_3. This

system is found to be very efficient for a wide range of benzylic alcohols, enabling high selectivity under mild reaction conditions (room temperature). Thus, it clearly mimics the Galactose oxidase natural performance. Unfortunately, the system show weaker activity against aliphatic primary and secondary alcohols, and copper complex yield should be reduced as well.

Appendix A. The structural data for CuL^{BAPP} have been deposited with the Cambridge Crystallographic Data Centre, the deposition number being CCDC 1494302 http://www.ccdc.cam.ac.uk/conts/retrieving.html, or from the Cambridge Crystallographic Data Centre, 12 Union Road, Cambridge CB2 1EZ, UK; fax: (+44) 1223-336-033; or e-mail: deposit@ccdc.cam.ac.uk.

Acknowledgments

Authors are grateful to the Institute for Advanced Studies in Basic Sciences (IASBS), Shiraz and the Slovenian Research Agency (Grant P1-0175) for their valuable help. AP also thank EN-FIST centre of Excellence, Ljubljana, Slovenia for using SuperNova diffractometer.

References

[1] R. Horton, L.A. Moran, G. Scrimgeour, M. Perry, D. Rawn, Principles of Biochemistry (4th ed.) Pearson Education (2005) 40–55.

[2] F. Thomas, Eur. J. Inorg. Chem. (2007) 2379–2404.

[3] N. Ito, S. E. V. Phillips, C. Stevens, Z. B. Ogel, M. J. McPherson, J. N. Keen, K. D. S. Yadav, P. F. Knowles, Nature, 350 (1991) 87–90.

[4] F. Michel, F. Thomas, S. Hamman, C. Philouze, E. Saint-Aman, J. L. Pierre, Eur. J. Inorg. Chem. (2006) 3684–3696.

[5] F. Escalettes, N. J. Turner, Chem. Bio. Chem. 9 (2008) 857–860.

[6] M. M. Whittaker, Y. Y. Chuang, J. W. Whittaker, J. Am. Chem. Soc. 115 (1993) 10029–10035.

[7] T. K. Paine, T. Weyhermuller, K. Wieghardt, P. Chaudhuri, Dalton Trans. (2004) 2092–2101.

[8] S. Itoh, S. Takayama, R. Arakawa, A. Furuta, M. Komatsu, A. Ishida, S. Takamuku, S. Fukuzumi, Inorg. Chem. 36 (1997) 1407–1416.

[9] P. Chaudhuri, M. Hess, U. Flörke, K. Wieghardt, Angew. Chem. Int. Ed. 37 (1998) 2217–2220.

[10] S. E. Balaghi, E. Safaei, M. Rafiee, M. H. Kowsari, Polyhedron 47 (2012) 94–103.

[11] T. Weyhermüller, R. Wagner, P. Chaudhuri, Eur. J. Inorg. Chem. 2011 (2011) 2547–2557.

[13] S. Oae, M. Yoshihara, W. Tagaki, Bull. Chem. Soc. Jpn. 40 (1967) 951–953.

[14] E. Safaei, T. Weyhermüller, E. Bothe, K. Wieghardt, Phalguni Chaudhuri, Eur. J. Inorg. Chem. 16 (2007) 2334–2344.

[15] A. R. Corcos, O. Villanueva, R. C. Walroth, S. K. Sharma, L. Bacsa, John, M. Kyle, C. E. MacBeth, J. F. Berry, J. Am. Chem. Soc. 138 (2016) 1796–99.

[16] S. E. Balaghi, E. Safaei, L. Chiang, E. W. Wong, D. Savard, R. M. Clarke, T. Storr, Dalton Trans. 42 (2013) 6829–6839.

[17] R. F. Munhá, R. A. Zarkesh and A. F. Heyduk, Dalton Trans.,42 (2013), 3751–3766.

[18] L. Chiang, A Kochem, O Jarjayes, J. D. Tim, H. Vezin, M. Sakaguchi, T. Ogura, M. Orio, Y. Shimazaki, Chem., Eur. J., 18 (2012) 14117–14127.

[19] Y. Shimazaki, D. Stack, T. Storr, Inorg. Chem. 48 (2009) 8383–8392.

[20] P. Chaudhuri, E. Bill, R. Wagner, U. Pieper, B. Biswas, T. Weyhermüller, Inorg. Chem. 47 (2008) 5549–5551.

[21] R. A. Sheldon, J. K. Kochi, Metal-Catalyzed Oxidation of Organic Complexs, Academic Press, (1991) 25–60.

[22] S. V. Ley, J. Norman, W. P. Griffith, S.P. Marsden, Synthesis 7 (1994) 639–666.

[23] M. Hudlicky, Oxidations in Organic Chemistry, ACS, (1990) 65–78.

[24] C. Jallabert, H. Riviere, Tetrahedron Lett. 14 (1977) 1215–1218.

[25] J. A. Halfen, V.G. Jr. Young, B. W. Tolman, Angew. Chem., Int. Ed. 35 (1996) 1687–1690.

[26] J. A. Halfen, B. A. Jazdzewski, S. Mahapatra, L. M. Berreau, E. C. Wilkinson, L. Jr. Que, W. B. Tolman, J. Am. Chem. Soc. 119 (1997) 8217–8227.

[27] A. Sokolowski, H. Leutbecher, T. Weyhermuller, R. Schnepf, E. Bothe, E. Bill, P. Hildebrandt, K. Wieghardt, J. Biol. Inorg. Chem. 2 (1997) 444–453.

[28] J. Muller, T. Weyhermuller, E. Bill, P. Hildebrandt, L. Ould–Moussa, T. Glaser, K. Wieghardt, Angew. Chem. Int. Ed. 37 (1998) 616–619.

[29] S. Bhaduri, N. Y. Sapre, Dalton Trans. 12 (1981) 2585–2586.

[30] N. Kitajima, K. Whang, Y. Morooka, A. Uchida, Y. Sasada, Chem. Commun. 20 (1986) 1504–1505.

[31] P. Chaudhuri, M. Hess, U. Florke, K. Wieghardt, Angew. Chem. Int. Ed. 37 (1998) 2217–2220.

[32] P. Gamez, I. W. C. E. Arends, J. Reedijk, R. A. Sheldon, Chem. Commun. (2003) 2414–2415.

[33] Agilent, CRYSALIS PRO, Agilent Technologies, Yarnton, England, 2011.

[34] A. Altomare, G. Cascarano, G. Giacovazzo, A. Guagliardi, J. Appl. Cryst. *27* (1994), 435–435.

[35] G. M. Sheldrick, Acta Cryst. Sect. A 64 (2008) 112–122.

[36] Z. Alaji, E. Safaei, L. Chiang, R. M. Clarke, C. Mu, T. Storr**,** Eur. J. Inorg. Chem. (2014) 6066–6074.

[37] E. J. Land, G. Porter, Trans. Faraday Soc. 59 (1963) 2016–2026.

[38] L. Dutta, A. Syamal, Elements of Magnetochemistry, Affiliated East-West Press PVT LTD, (1993) 6–10.

[39] C. Kittel, Introduction to Solid State Physics (8th ed), John Wiley & Sons (2005) 55–57.

[40] T. Storr, P. Verma, R. C. Pratt, E. C. Wasinger, Y. Shimazaki, T. D. P. Stack, J. Am. Chem. Soc. 130 (2008) 15448–15459.

[41] H. Chun, C. N. Verani, P. Chaudhuri, E. Bothe, E. Bill, T. Weyhermüller, K. Wieghardt, Inorg. Chem. 40 (2001) 4157–4166.

[42] A. Boettcher, H. Elias, E. G. Jaeger, H. Langfelderova, M. Mazur, L. Mueller, H. Paulus, P. Pelikan, M. Rudolph, M. Valko, Inorg. Chem. 32 (1993) 4131–4138.

[43] R. R. Gagne, C. A. Koval, T. J. Smith, M. C. Cimolino, J. Am. Chem. Soc. 101 (1979) 4571–4580.

[44] K. Asami, K. Tsukidate, S. Iwatsuki, F. Tani, S. Karasawa, L. Chiang, T. Storr, F. Thomas, Y. Shimazaki, Inorg. Chem. 51 (2012) 12450–12461.

[45] E. Safaei, L. Hajikhanmirzaei, B. Karimi, A. Wojtczak, P. Cotič, Y. Ill Lee, Polyhedron, 106 (2016) 153–162.

Table 1. Crystal data and structure refinement for **CuL^{BAPP}**

formula	$C_{28}H_{31}CuN_3O$
Fw (g mol^{-1})	489.10
crystal size (mm)	0.10 x 0.04 x 0.04
crystal color	red
crystal system	monoclinic
space group	*C*2/*c*
a (Å)	25.9272(9)
b (Å)	6.8885(3)
c (Å)	28.5350(9)
α (º)	90
β (º)	95.634(3)
γ (º)	90
V (Å^3)	5071.7(3)
Z	8
Calcd. density (g cm^{-3})	1.281
F(000)	2056
θ range (º)	2.87 – 27.48
No. of collected reflns.	23947
No. of independent reflns.	5805
R_{int}	0.0777
no. of reflns used	3408
no. parameters	313
$R[I > 2\sigma(I)]^a$	0.0585
wR_2 (all data)^b	0.1284
Goof , S^c	1.009
Max./min. residual electron	+0.30/-0.26

Table 2. Selected bond lengths [Å] and angles [^{0}] for **CuL^{BAPP}**

Cu1–O1	1.935(2)		O1–Cu1–N1	83.93(10)
Cu1–N1	1.940(3)		O1–Cu1–N2	173.64(11)
Cu1–N2	1.972(3)		O1–Cu1–N3	89.74(11)
Cu1–N3	1.878(3)		N1–Cu1–N2	94.09(11)
N1–C1	1.280(4)		N2–Cu1–N3	93.23(12)
N2–C7	1.420(4)		N1–C1–C2	125.9(3)
N2–C8	1.328(4)		N2–C7–C2	121.5(3)
N3–C14	1.324(4)		Cu1–N1–C1	126.1(2)
C1–C2	1.441(5)		Cu1–N2–C7	122.6(2)
C2–C7	1.408(5)		Cu1–N3–C14	130.2(3)

Table 3. The solvent effect (5 mL) at the benzyl alcohol oxidation with CuL^{BAPP} /Cs_2CO_3 (4/2 in mmol).

Solvent	**t / h**	**yield / %**
CH_3CN	6	49
THF	**4**	**100**
n-Hexane	6	37
Toluene	6	89

Table 4. The CuL^{BAPP} equivalencesCs_2CO_3 ratio influence (mmol) in THF (5 mL) at the benzyl alcohol oxidation.

$n_{(CuLBAPP)}/n_{(Cs2CO3)}$	Solvent		
		t / h	yield / %
2/2	THF	4	45
3/2	THF	4	62
4/2	THF	**4**	**100**
5/2	THF	4	100

Table 5. Different basic agents at the alcohol oxidation with 4 mmol of CuL^{BAPP} in THF.

n/mmol Base	Solvent		
		t / h	yield / %
1 $NaNO_2$	THF	24	2
1 KOH	THF	6	47
1 NEt_3	THF	24	22
1 Cs_2CO_3	THF	4	48
2 Cs_2CO_3	THF	**4**	**100**
3 Cs_2CO_3	THF	4	100

Table 6. The result of blank test for oxidation of benzyl alcohol with similar catalytic system

Catalytic system	t / h	yield / %
$Cu(OAc)_2$ /Cs_2CO_3	24	26
$Cu(OAc)_2$ /Cs_2CO_3/HL^{BAP}	4	85

Table 7. Different alcohols applied for their oxidation to corresponding aldehyde in THF, catalyzed by CuL^{BAPP} in a presence of Cs_2CO_3 as a base and O_2 as an oxidant.

	Substrate	**t / h**	**yield / %**
1	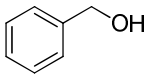	4	100
2	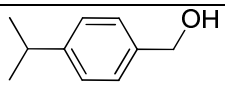	4	90
3	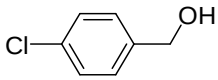	6	96
4	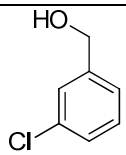	8	92
5	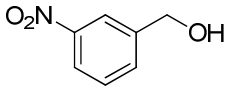	24	81
6	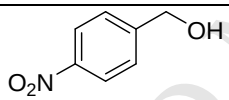	24	75
7	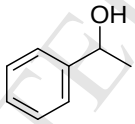	24	76
8	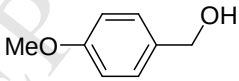	24	64
9	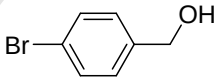	24	23
10	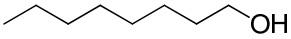	24	-

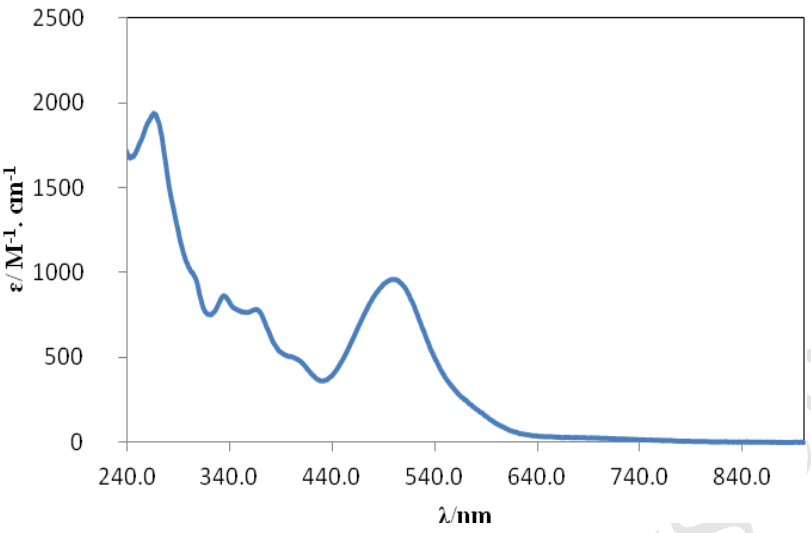

Figure 1. Electronic absorption spectra of **CuL**$^{\mathbf{BAPP}}$

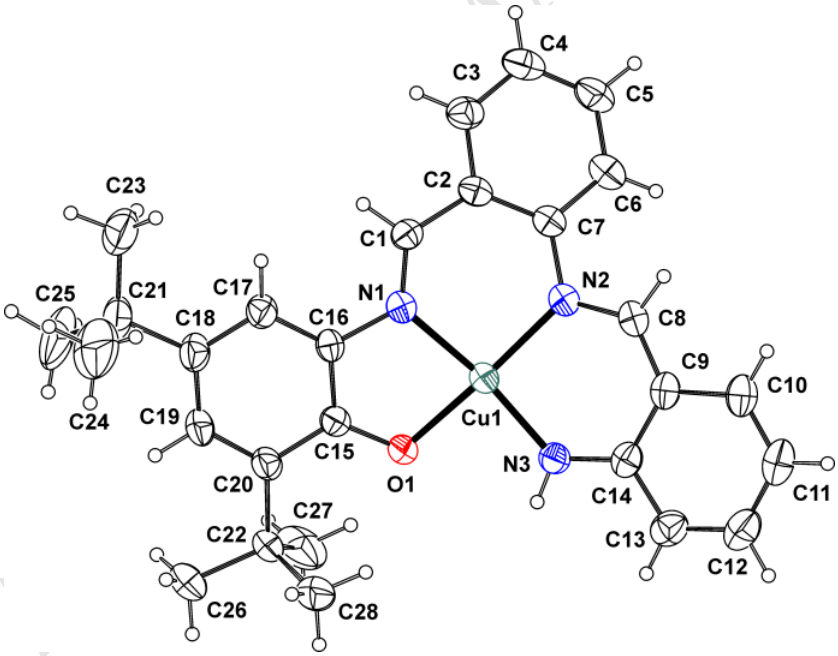

Figure 2. ORTEP diagram and atom labeling scheme for complex **CuL**$^{\mathbf{BAPP}}$

Ellipsoids are plotted at 30% probability level. Hydrogen atoms are omitted for clarity.

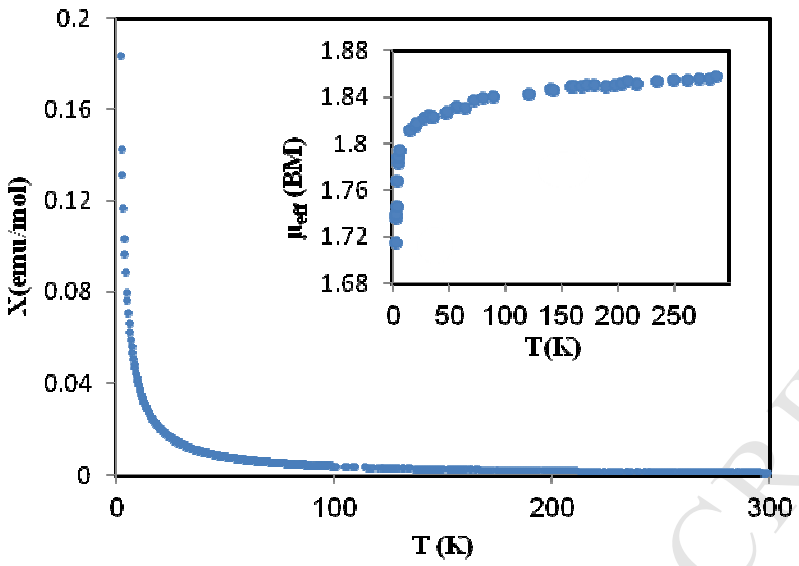

Figure 3. Temperature dependent susceptibility χ(T) and the effective magnetic moment μ_{eff}(T) (inset) of **CuL^{BAPP}** measured in a magnetic field of H = 1 kOe.

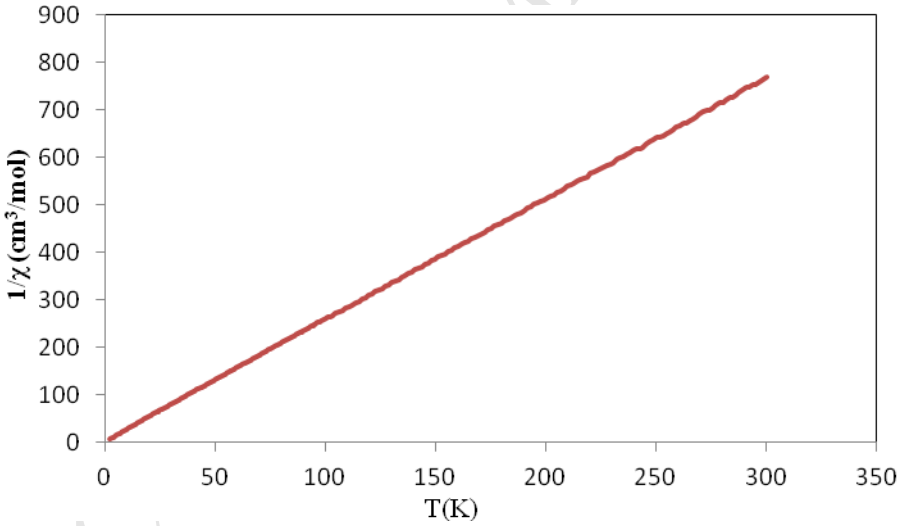

Figure 4. χ^{-1}(T) of **CuL^{BAPP}** measured in a magnetic field of H = 1 kOe.

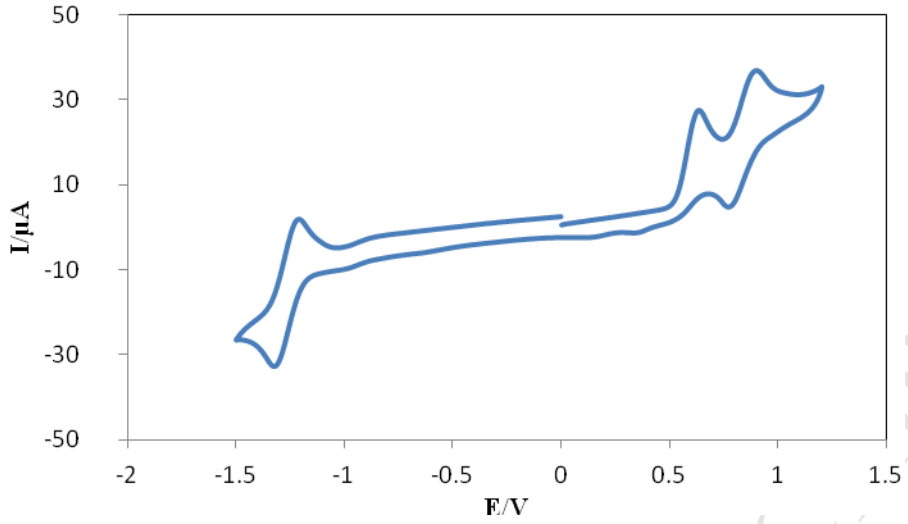

Figure 5. Cyclic voltammogram of **CuL**$^{\mathbf{BAPP}}$ in CH_2Cl_2 at RT. (sc 25 mVs^{-1}).

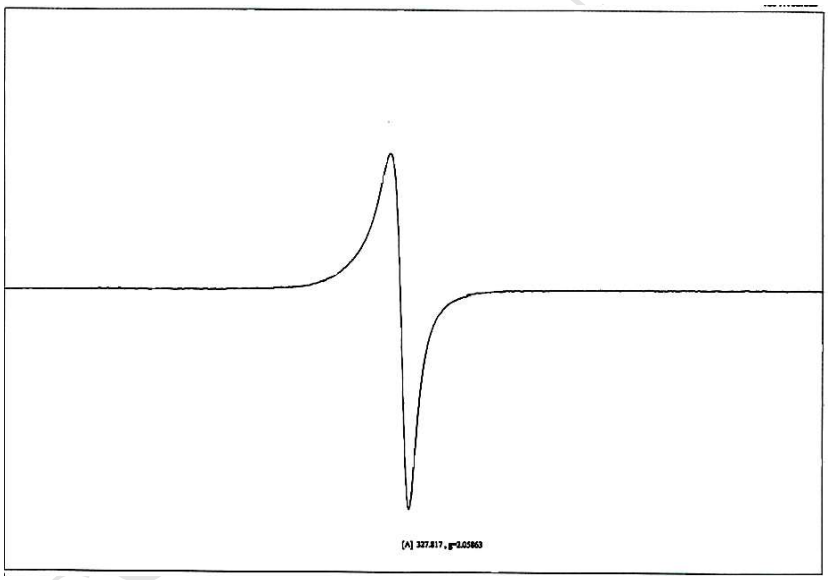

Figure 6. EPR spectrum of **CuL**$^{\mathbf{BAPP}}$

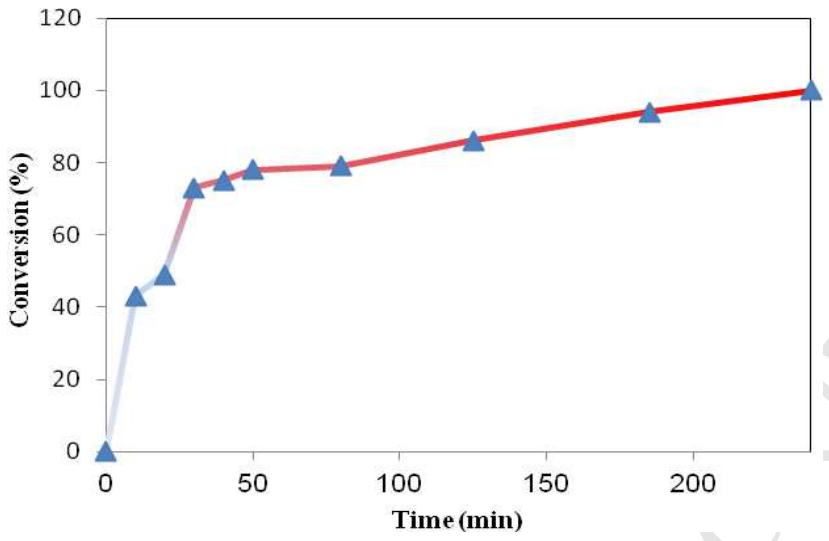

Figure 7. Time screening of benzyl alcohol oxidation alcohol with **CuL^{BAPP}**

Research Highlights

- Copper(II) complex of tetra-dentate *o*-aminophenol-based.
- Excellent galactose oxidases mimic system.
- Aerobic oxidation of alcohols.